Express diagnostics of WWER fuel rods at nuclear power plants

S.V.Pavlov, S.V.Amosov, S.S.Sagalov and A.N.Kostyuchenko

Higher safety and economical efficiency of nuclear power plants (NPP) call for a continuous design modification and technological development of fuel assemblies and fuel rods as well as optimization of their operating conditions. In doing so the efficiency of new fuel introduction depends on the completeness of irradiated fuel data in many respects as well as on the rapidity and cost of such data obtaining. Standard examination techniques of fuel assemblies (FA) and fuel rods (FR) intended for their use in hot cell conditions do not satisfy these requirements in full extent because fuel assemblies require preliminary cooling at nuclear power plants (NPP) to provide their shipment to the research center. Expenditures for FA transportation, capacity of hot cells and expenditures for the examined fuel handling do not make it possible to obtain important information about the condition of fuel assemblies and fuel rods after their operation.

In order to increase the comprehensiveness of primary data on fuel assemblies and fuel rods immediately after their removal from the reactor, inspection test facilities are widely used for these purposes. The inspection test facilities make it possible to perform non-destructive inspection of fuel in the NPP cooling pools [1]. Moreover these test facilities can be used to repair failed fuel assemblies.

At present Russia has got a stand for inspection and repair of fuel assemblies TVSA WWER-1000 for the Kalinin NPP. The Westinghouse test facility at Temelin NPP is being upgraded to carry out the inspection and repair of TVSA-T WWER-1000. The TV inspection system is used for visual inspection and measurement of FA dimensions. The ultrasonic inspection method is used to detect failed fuel rods in the fuel assembly. The stand for inspection and repair at the Kalinin NPP is also equipped with the eddy current system for eddy current testing of FR claddings.

The design of the stand for inspection and repair of alternative fuel assemblies TVSA WWER-1000 will make it possible to use complementary methods of examination for fuel assemblies and fuel rods such as measurement of the oxide film thickness on the outer surface of FR cladding, diametrical cladding-fuel gap, cladding diameter etc. These methods have been successfully used at RIAR for examination of irradiated fuel assemblies WWER-440 and WWER-1000 for many years. They proved their reliability and efficiency and could be easily accommodated for underwater conditions in the NPP cooling pools.

The ultrasonic testing of failed fuel rods inside the fuel assembly is based on the detection of water in the fuel -cladding gap of fuel rod that penetrated there due to fuel rod

failure [2, 3]. Ultrasonic waves are generated with the detector in the cladding of fuel rod from the upper end plug. These waves propagate over the cladding up to the lower end plug of fuel rod, reflect and are detected with the same detector as soon as they have passed from the bottom upwards in the cladding (Fig.1a). In doing so the corresponding signal is found on the oscillogram (Fig.1b).

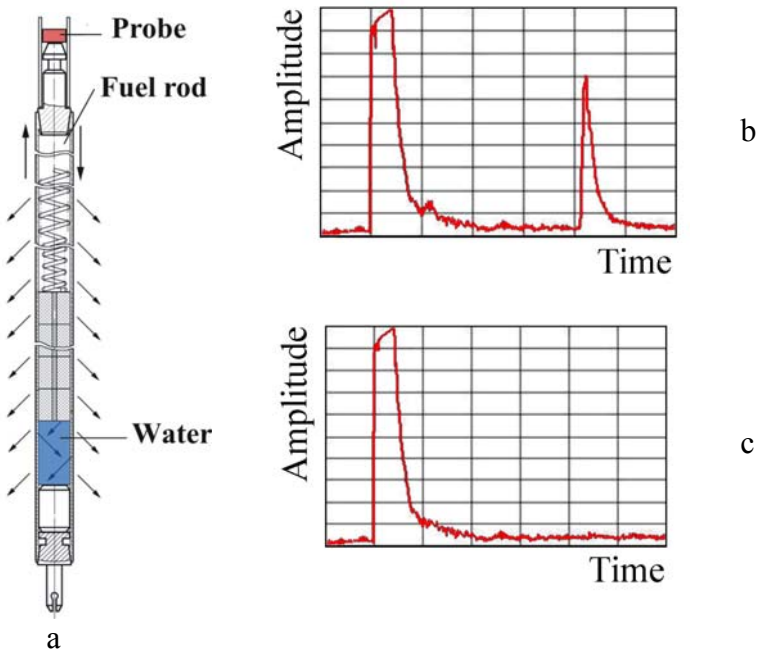

Fig. 1. Ultrasonic testing of failed fuel rods: 1 – schematic representation of fuel rod and fuel rod being tested; 2 – oscillogram of failed fuel rod; 3 – oscillogram of fight fuel rod.

When the water is present under the cladding of fuel rod, the wave energy is dissipated in larger quantity as compared with the fight fuel rod and as a result of this the amplitude of sensed signal decreases. Usually the signal can not be seen on the oscilllogram because its amplitude is lower than the noise level (Fig.1c).

The sensitivity of this method can be represented as a relationship between the amplitude of sensed signal for the fight fuel rod $\mathbf{A_I}$ and amplitude of signal for failed fuel rod $\mathbf{A_F}$. As one can see in paper [3], the amplitude relation can be presented in the following way:

$$A_I / A_F = \text{const} \ \exp\left[\mathrm{V}/\overline{\mathrm{S}}(\mathrm{z})\right], \qquad (1)$$

where: **V** – volume of water in the cladding-fuel gap;

$\overline{S}(z)$ – average area of the cladding-fuel gap for the segment of fuel rod filled with water.

The sensitivity of this method can be described with two cofactors (1). The first cofactor depends on the parameters of ultrasonic waves or to be more exact it depends on the wave attenuation factor. Wave attenuation happens due to the energy radiation in the environment surrounding the fuel rod cladding. The second exponential cofactor depends on the parameters

of failed fuel rod i.e. the quantity of water in the fuel -cladding gap and this gap size.

Two conditions must be met to provide a reliable detection of failed fuel rods. The first condition resides in the fact that the sensed signal must be several times higher than the noise level of electronics for fight fuel rods. The second condition resides in the fact that the sensitivity of method must be as high as possible but all other things being equal **V=const,** $\overline{S}(z)$**=const**. These conditions were used as a basis to choose the optimal parameters of method for the WWER fuel rods. Fig.2 demonstrates empirical relation of A_F/A_I and water content under the cladding of dummy fuel rods WWER-1000 with the diametrical cladding-fuel gap of ~220 μm that corresponds to the initial gap in the non-irradiated WWER fuel rods. The results of these experiments are well described with the exponential relation:

$$A_F/A_I = \exp[-17.5V]. \qquad (2)$$

The exponential relation (2) agrees with the theoretic function (1) and this proves the validity of the physical model.

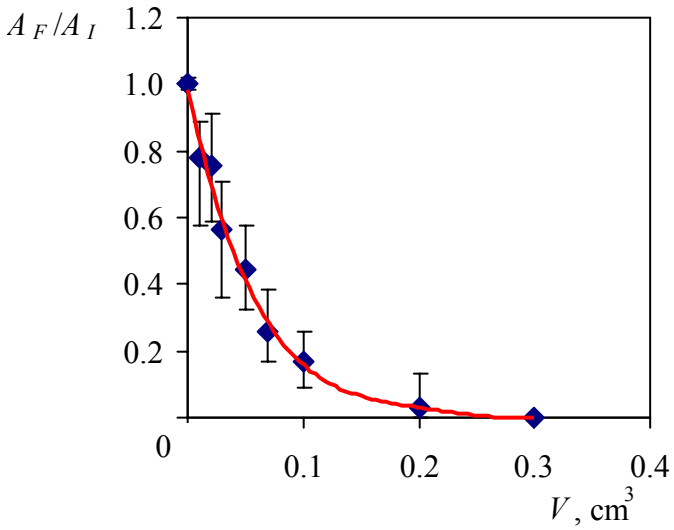

Fig. 2. Amplitude of the sensed signal against the water volume in the fuel –cladding gap of the dummy defect VVER FR

Eight leaking fuel assemblies VVER-440 and WWER-1000 with a burnup of 13.8 up to 37.5 MW·day/kgU were used to check this method. These fuel assemblies were examined at RIAR. The results of check proved a high reliability degree of this method within the specified range. All failed fuel rods were correctly identified.

There is a possible reason that can limit the use of this method. The reason resides in a tight fuel –cladding contact in fuel rods. It is well known that the tight fuel –cladding contact in the WWER-440 and WWER-1000 fuel rods begins at burnups of 40÷45MW·day/kgU. That is why it will be necessary to check the efficiency of this method with the use of the

WWER fuel assembly with burnups of ~40 MW·day/kgU and higher in order to determine the scope of its applicability.

A special manipulator with 52 probes (Fig.3) was developed and tested to detect failed fuel rods in the TVSA WWER-1000.

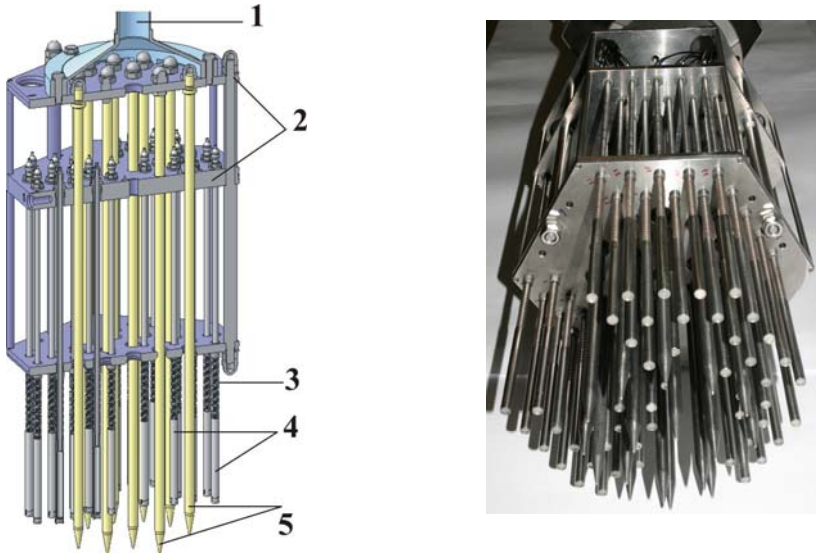

a b

Fig.3. Sketch of the manipulator (a) and appearance of the lower part of the manipulator (b): 1-rod; 2-frame; 3-spring; 4-ultrasonic probes; 5-guiding pins.

The manipulator is positioned at the upper part of TVSA as soon as the head piece has been removed. All the fuel rods of TVSA are tested by moving the manipulator six times and by turning it through an angle of 60° relative to the vertical axis. The probes are spring-loaded and can be moved in the vertical direction according to the length and difference in height of fuel rods in the TVSA. The fifty two probes are scanned in the automatic and manual modes.

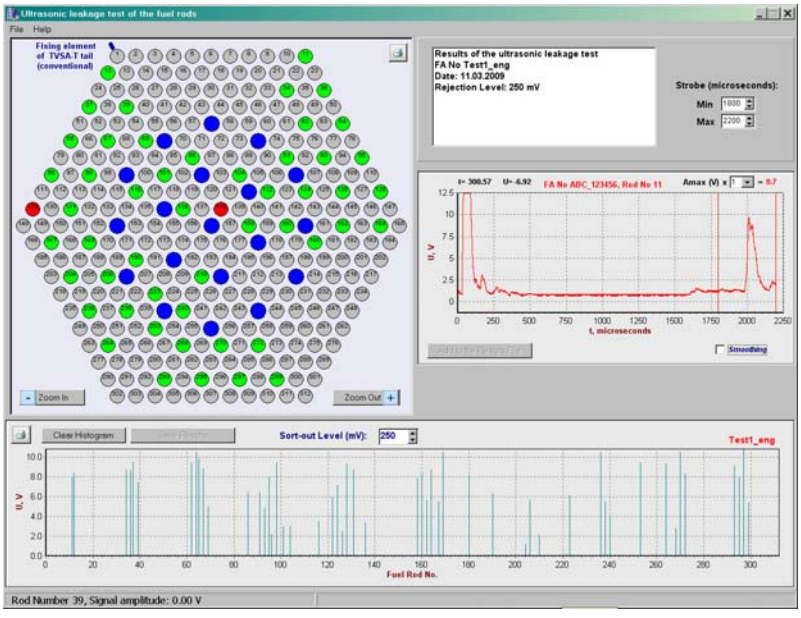

Fig.4. The main window of computer program

The software enables the automatic rejection of fuel rods whose signal amplitudes are lower as compared with the predetermined value, marking these fuel rods on the TVSA schematic view and logging the results of testing. Fig.4 shows the main window of computer program as an example.

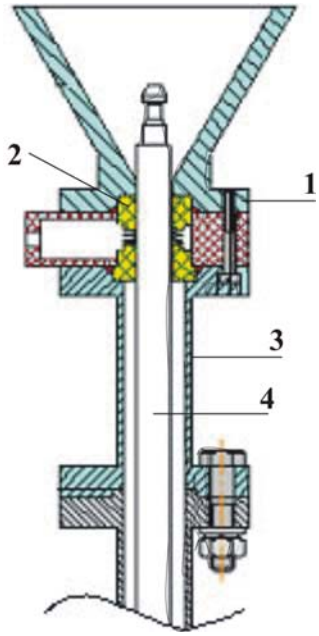

Fig.5. Positional of the eddy current probe and fuel rod under examination: 1-eddy current probe body; 2-measuring coil; 3-container for fuel rod; 4-fuel rod.

A pulsed eddy current testing [4] was used to reveal the defects in the cladding of fuel rods. The fuel rod withdrawn from the bundle is placed into the container with a special tool. There is an eddy current probe at the upper part (Fig.5). It is coaxial in shape. The fuel rod is pulled upward across the eddy current probe and in doing so, the fuel rod cladding defectoscopy (defect detection) is performed.

The sensing coil of the probe comprises the inductive transmitting coil and two measuring induction coils. This method is based on the analysis of interaction between the external electromagnetic field with the electromagnetic field of eddy currents which are induced with the inductive transmitting coil in the electroconductive cladding of fuel rod due to the current impulse penetration.

Fig.6 demonstrates the eddy current probe signals from the artificially applied defects in the non-irradiated WWER FR cladding. The table given below describes the types and dimensions of these artificially applied defects in the cladding.

These defects are identified (external defect, internal defect and thorough defect) based on the hodograph shape, its amplitude, and angular displacement. As one can see in Fig.6, a thorough hole 0.4 mm in diameter is detected with confidence by the eddy-current detector but a special adjustment of the eddy-current detector for through defects makes it possible to detect thorough defects to be 0.25 mm in diameter.

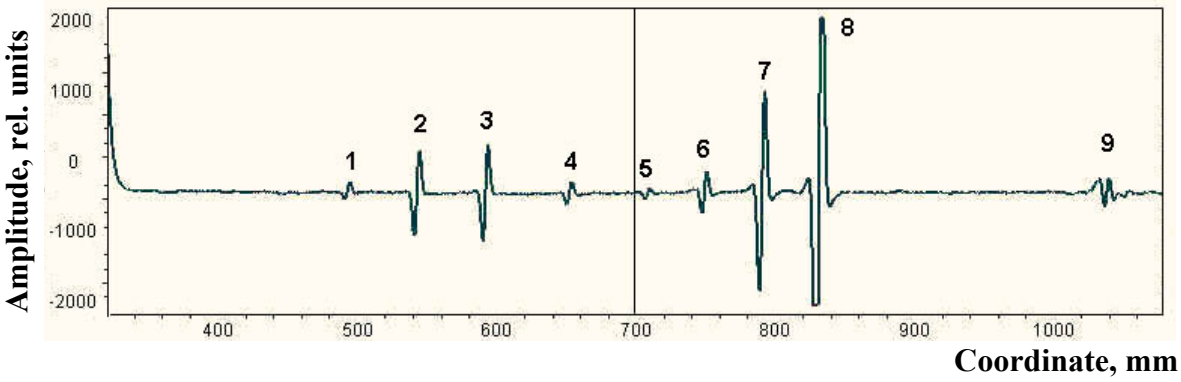

Fig.6. Diagram of the eddy-current probe signals from the artificially applied defects

Table

Characterization of the artificially applied defects

Defect No.	Defect description and its nominal dimensions
1	External blind hole, 0.7 mm in diameter, 0.3 mm deep
2	External circular mark, 0.06 mm deep, 0.08 mm wide
3	External circular mark, 0.10 mm deep, 0.14 mm wide
4	External blind hole, 0.7 mm in diameter, 0.5 mm deep
5	Through hole, 0.4 mm in diameter
6	Through hole, 0.8 mm in diameter
7	Through hole, 1.5 mm in diameter
8	Through hole, 2.5 mm in diameter
9	Internal circular mark, 0.20 mm deep, 0.25 mm wide

By way of illustration Fig.7a demonstrates the results of defectoscopy for the WWER-1000 FR with the part-thorough debris-defect in the cladding. The defect was applied artificially in the form of crescent (Fig.7 b, c) and measured ~5.0x0.2 mm and ~0.57 mm deep. The signal magnitude produced by the defect is dozens of times higher as compared with the noise level (Fig.7a) and this clearly points to the fact that the sensitivity of method is high. This method of testing makes it possible to detect the secondary defects such as hydride precipitates in the cladding wall along with the primary thorough defect in the cladding of defect fuel rods.

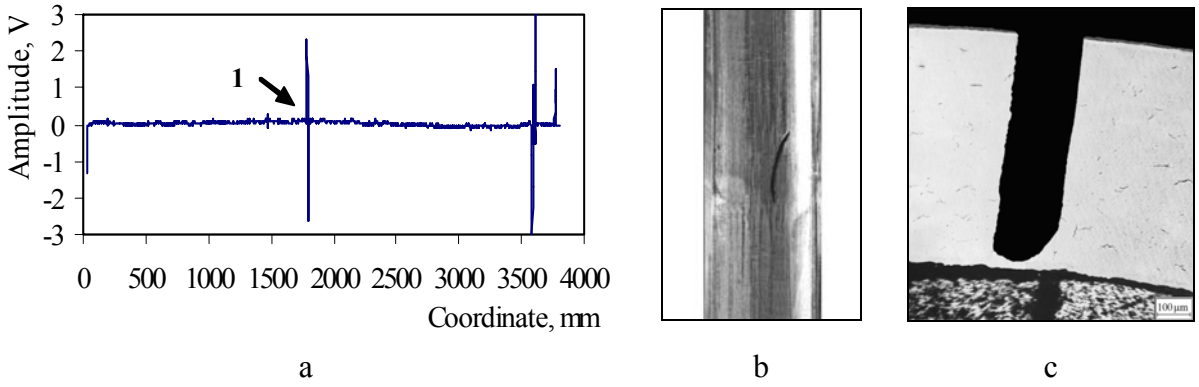

Fig.7. Results of the eddy-current defectoscopy of the FR cladding (a), outer appearance (b) and cross-section of the cladding with the part-through debris-defect: 1-signal of the debris-defect.

Fig.8a demonstrates an eddy-current diagram of the defect WWER-1000 fuel rod. There is a through debris-defect of the cladding in its lower part (Fig.8b). As for the upper part, there are clusters of the “sunburst”-type hydrides on the cladding wall (Fig.8c).

Except for the detection of defects in the cladding of fuel rods, the defectoscopy by means of the pulsed eddy-current method makes it possible to reveal local changes in the cladding diameter.

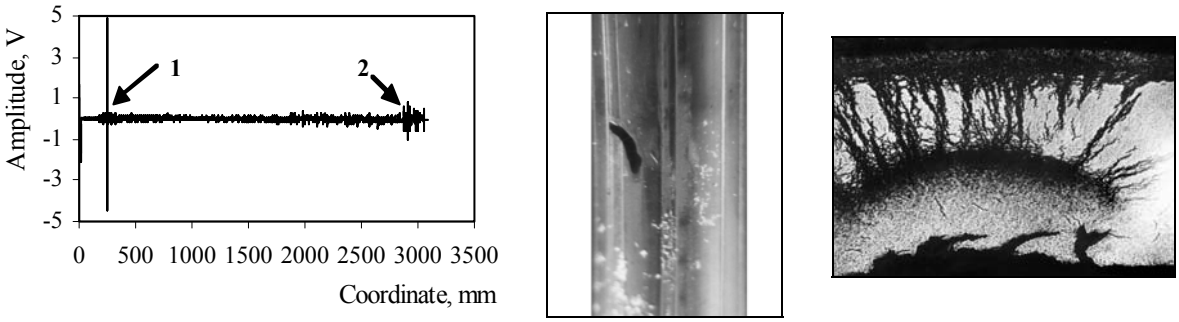

Fig.8. Results of eddy-current defectoscopy of the defect fuel rod: a-eddy-current diagram; b-appearance of the debris-defect; c-cladding microstructure in the region of the secondary defects; 1-signal of the debris-defect; 2-signals of the secondary internal defects.

The diameter of fuel rod cladding decreases under operation in the reactor due to thermal creep but the diameter of fuel pellets increases due to swelling. As soon as the fuel rod has achieved a specific fuel burnup, the diametrical fuel-to-cladding gap disappears. In doing so, fuel continues swelling and as a result the cladding undergoes the plastic strain and its diameter increases that is so-called reverse strain of the cladding.

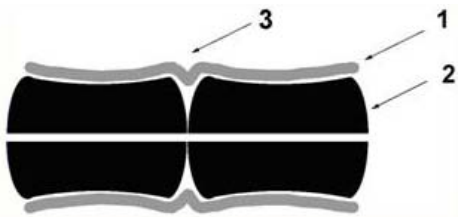

Fig.9. Formation of goffers: 1-cladding; 2- fuel pellet; 3-goffers.

The pellet-cladding interaction results in the local decrease of diameter that is so-called "goffering" (Fig.9) of the cladding at the places of pellet junctions. By way of illustration Fig.10 demonstrates the results of measurement by profilometry and defectoscopy by means of eddy-current method for the WWER-1000 FR cladding with a burnup of ~55 MW·day/kgU. As may be well seen from the profilogram (profile diagram), there is a reverse strain of the cladding in the center of fuel rod (Fig.10a). In this case the signals with the time interval equal to the fuel pellet length can be well seen on the eddy-current diagram.

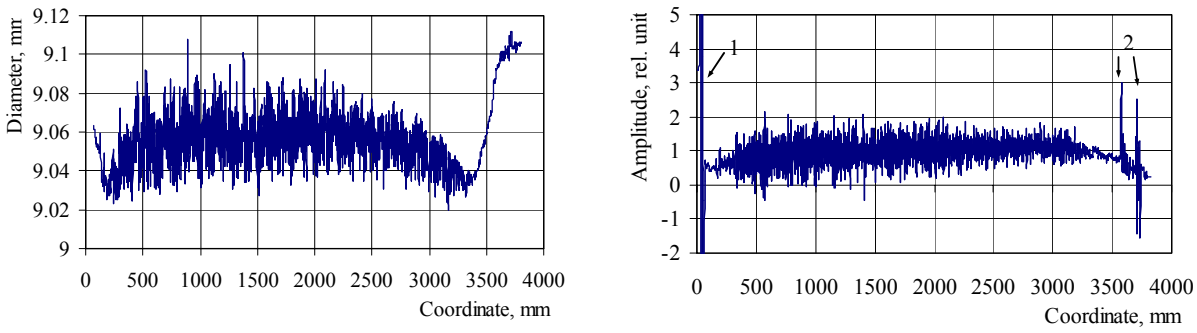

Fig.10. Results of diameter measurement (a) and defectoscopy by means of eddy-current method (b) of the WWER -1000 FR with a burnup of 55 MW·day/kgU: 1-signal of the plug; 2-signals of the fixing mechanism

As the burnup increases, the goffers increase in size also and the magnitude of the eddy-current signals produced by the gofferes increases respectively (Fig.11).

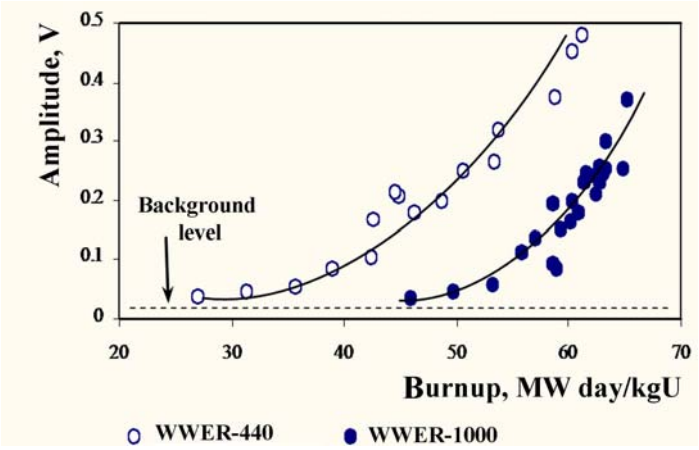

Fig.11. Magnitude of the eddy-curent signal against fuel burnup

In doing so, the analysis of the results of the eddy-current testing of claddings makes it possible to determine the time of the tight cladding-fuel contact as well as to estimate the degree of cladding-fuel interaction. The eddy-current testing has been used at RIAR as an express testing method of cladding integrity for many years. It is used during the post-irradiation examinations of spent fuel assemblies WWER-440 and WWER-1000. This testing method was used for examination of 47 spent WWER fuel assemblies in total. But there were 16 failed spent fuel assemblies among them.

To determine the value of diametrical cladding-fuel gap for the WWER fuel rods, a non-destructive testing method was developed and has been successfully used at RIAR. This method is based on the local compression of the cladding till it comes in contact with the fuel column that is followed by the analysis of "force"-"cladding deformation" diagram [5, 6].

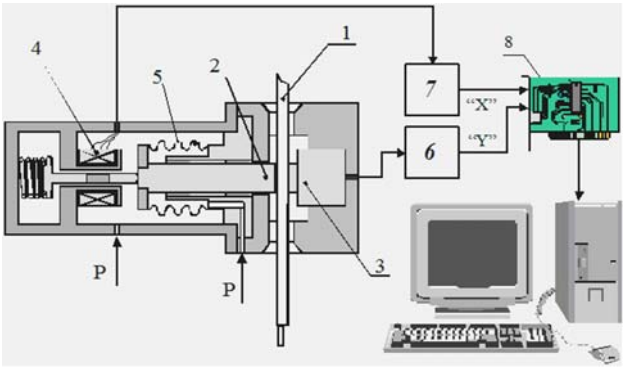

Fig.12. Scheme of diametrical gap measuring equipment: 1-fuel rod; 2-loading pin; 3-load sensor; 4-displacement transducer; 5-bellows; 6-charge amplifier; 7-amplifier; 8-analog-to-digital converter.

Fig.12 demonstrates the scheme of this facility. The fuel rod under examination is placed between the loading pin of 20 mm diameter and piezoelectric load sensor. A pneumatic system is used to apply a load to the fuel rod cladding with the help of loading pin. The loading pin displacement is measured with the electromagnetic sensor. The maximum force to be applied to the cladding should be 1200 N and below.

Fig.13 demonstrates a typical diagram "force"-"cladding deformation" under loading conditions ("forward trend", pointers are upward) and removal of load ("reverse trend", pointers are downward) of the WWER fuel rod. As for the forward trend, the load curve (at zero value of the diametrical gap) has a linear range of 0-1 that corresponds to the elastic deformation of the cladding until one of its sides comes in contact with the fuel. The length of

this region depends on the position of fuel column relative to the cladding and it can vary significantly at the same value of the diametrical gap.

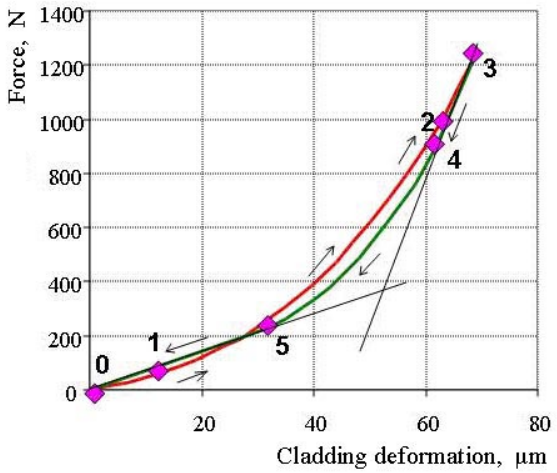

Fig.13. Typical diagram "force"-"deformation"

A nonlinear relation between the cladding deformation and loading force in the range of 1-2 can be explained as the beginning of deformation of the cladding wall material, centering of fuel pellets, and possible displacement of their fragments. The relationship between the deformation and loading approaches to the linear one and corresponds to the combined deformation of the cladding walls and pellets that are in a tight contact with them within a range of 2-3 above the transition interval.

Since the displacement of pellets and their fragments seems to be inelastic, the above-mentioned linear ranges are more pronounced (ranges 3-4 and 5-0) with regard to the reverse trend of the load curve and the length of transition interval between them (range 4-5) decreases as compared with the forward trend. That is why the diametrical gap is estimated by the reverse trend based on the projection of linear range 5-0 of the load curve into the horizontal axis (Fig.13).

Due to the fact that the cladding of fuel rod is deformed in a 20 mm long region (the loading pin diameter), it is impossible to refer the gap being measured to any other gap that has been measured with the use of standard technique such as optical metallographic examination of the metallographic cross-section that is cut out from the same region of fuel rod.

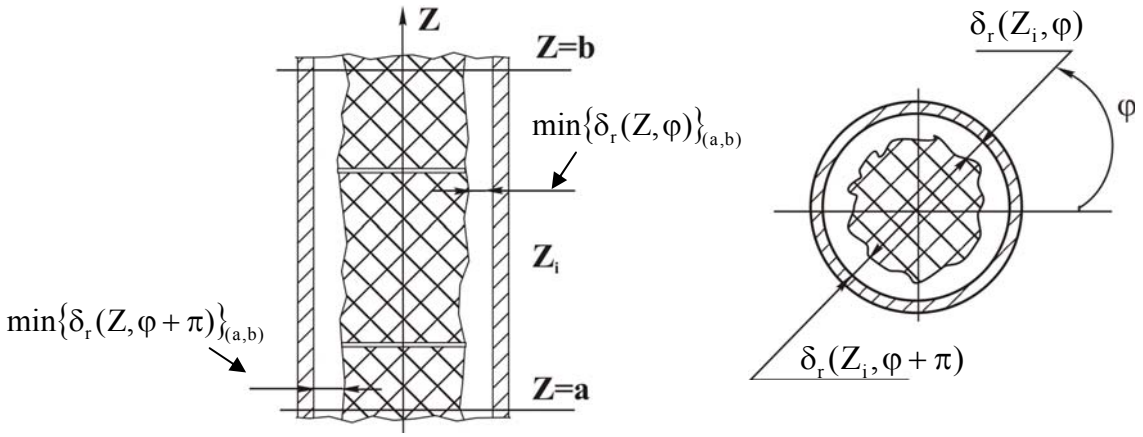

Fig.14. Schematic representation of the longitudinal section (a) and cross-section (b) of fuel rod

The longitudinal section and cross-section of fuel rod are represented schematically in Fig.14. Let us assume that the cladding is deformed in the region of length (a, b). We assume that the fuel pellets are not fragmented and immovable relative to each other and relative to the cladding but the radial fuel-cladding gaps disappear under deformation.

Then diametrical gap $\delta_{ND}(\varphi_i)_{(a,b)}$ that is produced non-destructively within the cladding region (a, b) and in the direction of azimuth coordinate φ_i is determined as a sum of minimal radial gaps in the same region with azimuth coordinates φ_i and $\varphi_i+\pi$:

$$\delta_{ND}(\varphi_i)_{(a,b)} = \min\{\delta_r(Z_i,\varphi_i)\}_{(a,b)} + \min\{\delta_r(Z_i,\varphi_i+\pi)\}_{(a,b)}, \quad (3)$$

where $\delta_r(Z_i,\varphi_i)$; $\delta_r(Z_i,\varphi_i+\pi)$ - radial gaps at the cross-section with coordinate Z_i and with azimuth coordinate φ_i, $a \le Z_i \le b$.

Diametrical gap $\delta_{MG}(Z_i,\varphi_i)$ for any metallographic cross-section with coordinate Z_i is found in the following way for azimuth coordinate φ_I:

$$\delta_{MG}(Z_i,\varphi_i) = \delta_r(Z_i,\varphi_i) + \delta_r(Z_i,\varphi_i+\pi). \quad (4)$$

So when the metallographic examinations are performed, the diametrical gap is determined as a sum of radial gaps which are in the plane of FR cross section.

As for the non-destructive examinations, the diametrical gap is determined as a sum of the minimal radial gaps which can be present at different heights within FR region (a, b).

Formulas (3) and (4) allow for the comparative appraisal of results obtained with the use of non-destructive method and optical metallography.

Diametrical gap $\delta_{ND}(\varphi_i)_{(a,b)}$ measured non-destructively for any arbitrary azimuth coordinate φ_i should not be higher than the minimum value of the gap calculated for the same coordinate φ_i and for all the possible cross-sections within the region (a, b):

$$\delta_{ND}(\varphi_i)_{(a,b)} \le \min\{\delta_r(Z_i,\varphi_i) + \delta_r(Z_i,\varphi_i+\pi)\}_{(a,b)}. \quad (5)$$

As it logically follows from inequation (5):

$$\min\{\delta_r(Z_i,\varphi_i) + \delta_r(Z_i,\varphi_i+\pi)\}_{(a,b)} \le \delta_{MG}(Z_i,\varphi_i) \le \delta_{MG}(Z_i,\varphi_i)^{\max}_{(a,b)}, \quad (6)$$

where $\delta_{MG}(Z_i,\varphi_i)$ is the diametrical gap measured at the metallographic cross-section with arbitrary coordinate Z_i and coordinate φ_i;

$$\delta_{MG}(Z_i,\varphi_i)^{\max}_{(a,b)} = \max\{\delta_{MG}(Z_i,\varphi_i)\}^{\max}_{(a,b)}.$$

So the gap value determined non-destructively for FR region (a, b) and in azimuth direction φ_i can not be higher than the maximum gap value determined with the help of optical metallography for any metallographic cross-section cut out from this region for all the possible values φ_i: $0 \le \varphi_i \le \pi$.

In doing so the non-destructive method provides the integral characteristic of the

diametrical gap for FR length (a, b) in azimuth direction φ. This characteristic can be considered as an estimation of the minimal gap value at any cross-section of this FR region with the same azimuth coordinate.

The results of non-destructive testing and optical metallography were compared for 15 fragments of the WWER-1000 fuel rods with a burnup of 20 up to 50 MW·day/kgU. One metallographic section was cut out from each fragment to measure the minimal, average and maximum diametrical gaps. The diametrical gap was estimated non-destructively in one direction and the results of measurements were not related to the azimuth coordinate.

Fig. 15 demonstrates the comparison of data obtained with help of two methods.

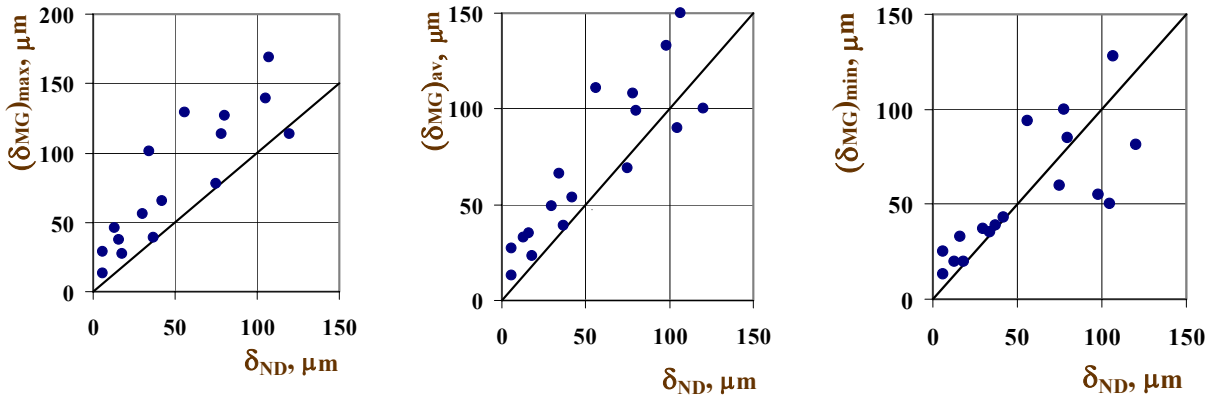

a b c

Fig.15. Comparison between the non-destructive measurement results (δ_{ND}) and: a - maximum (δ_{MG}); b - average (δ_{MG}); c - minimum (δ_{MG}) values of gap determined for the FR metallographic sections

The maximal values of diametrical gap measured for the metallographic sections are above the line of equal values measured non-destructively (Fig.15a). This fact proves the validity of inequation (6).

Referring to Fig.15, the diametrical gap values estimated non-destructively are in the best agreement with the minimal values of gaps obtained for the metallographic sections (Fig.15c).

A great number of examined fuel rods prove the validity of gap estimation with the help non-destructive testing. Fig.16 shows the averaged gap values obtained with the use of non-destructive method against fuel burnup. These data are in a good agreement with the results of metallographic examination for the metallographic cross-sections, which are obtained within the same range.

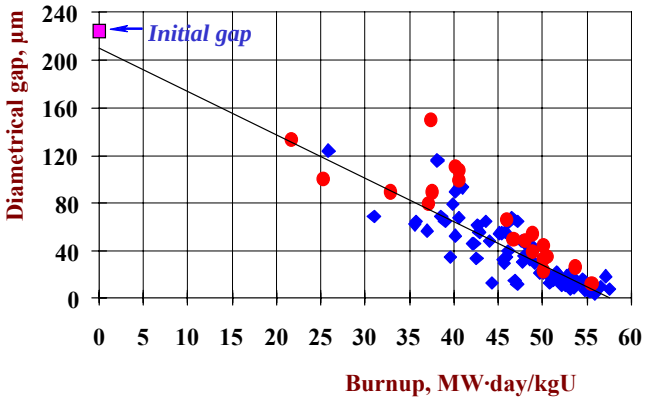

Fig.16. Diametrical fuel-cladding gap in the VVER-1000 fuel rods as a function of fuel burnup: ◆ - non-destructive testing; ● - optical metallography.

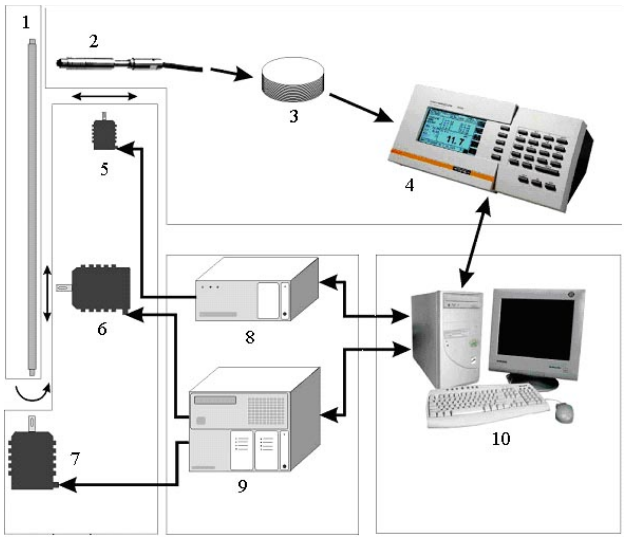

Fig.17. Equipment for oxide film thickness measurement: 1-fuel rod; 2-eddy-current probe; 3-signal amplifier; 4-signal processing unit; 5, 6, 7-stepper motors; 8, 9-stepper motor controller; 10-computer

The express non-destructive method of oxide film thickness measurement on the surface of WWER FR claddings is based on the eddy-current concept of thickness measurement. This facility (Fig.17) comprises the miniaturized eddy-current probe that is attached to the FR cladding with special fasteners and positioned perpendicular to the cladding surface [7]. A scanning system enables the probe movement along the fuel rod and fuel rod turning relative to the probe.

It was possible to estimate the error of the oxide film thickness measurement based on the results of testing with the use of special specimens. The error made up ±4 μm. As an example, Fig.18 demonstrates the results of the oxide film thickness measurement for the irradiated WWER fuel rods with the claddings made of alloys E110 and E635 and the results obtained for the metallographic cross-sections with the use optical metallography [8]. The results obtained with the use of two methods were compared. This comparison proves their good agreement.

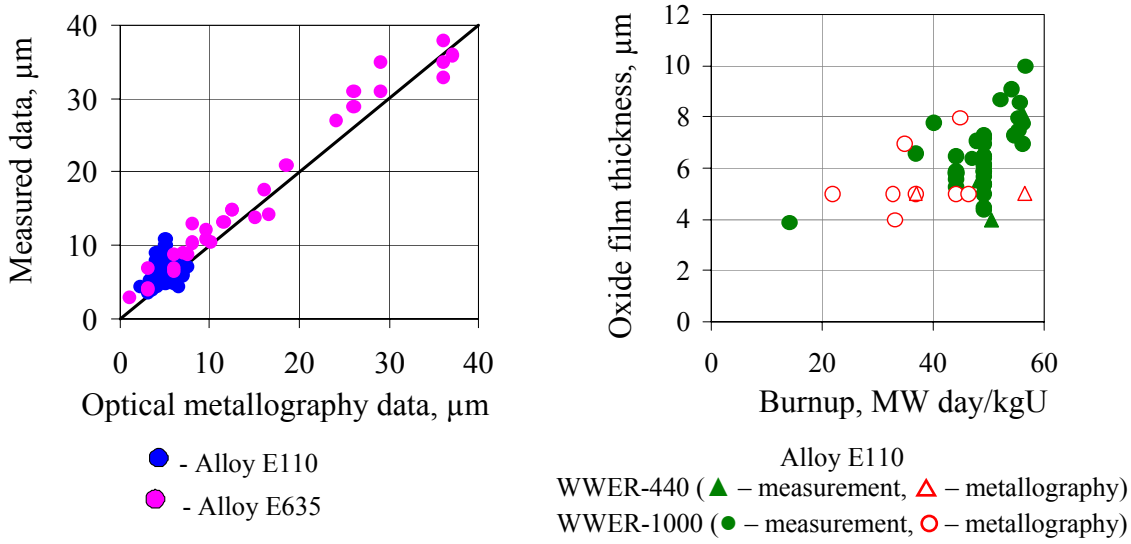

Fig.18. Results of method testing with the use of WWER fuel rods

The use of express non-destructive method of oxide film thickness measurement for PIE of WWER fuel rods made it possible to increase the E110 and E635 cladding oxidation database several times. Moreover, this method made it possible to select the regions of fuel rods more qualitatively for further metallographic examinations.

Conclusion

1. The ultrasonic testing of failed fuel rods inside the fuel assembly was developed for stands of inspection and repair of TVSA WWER-1000 for the Kalinin NPP and Temelin NPP.
2. This method was tested for eight leaking fuel assemblies WWER-440 and WWER-1000 with a burnup of ~14 up to 38 MW·day/kgU. The ultrasonic testing proved its high degree of reliability and efficiency.
3. The defectoscopy by means of the pulsed eddy-current method was adapted for the stand of inspection and repair of TVSA WWER-1000 for the Kalinin NPP. This method has been used at RIAR as an express testing method of FR claddings during the post-irradiation examinations of fuel assemblies WWER-440 and WWER-1000. This testing method was used for examination of 47 spent WWER fuel assemblies in total. But there were 16 failed spent fuel assemblies among them.
4. Methods of oxide film thickness measurement and fuel-cladding gap measurement in the WWER fuel rods have been successfully used for examination of the WWER fuel in hot cells. They can be easily adapted for use under water and can be recommended for adoption at stands of inspection and repair of TVSA WWER-1000.

References

1. S.V. Pavlov. Test facilities for inspection, repair and upgrade of fuel assemblies. Review. Dimitrovgrad, RIAR, 1996.

2. S.V. Pavlov, I.M. Vorobei, and T.M. Shalaginova. Investigation of acoustic path of ultrasonic methods of determining untight fuel elements included in fuel assembly. RIAR-1(856). Dimitrovgrad, 1997. (Rus.).

3. S.V. Pavlov. Detection of failed fuel rods in the VVER and RBMK fuel assemblies and results of detection method adoption. Atomnaya Energiya, 2009, Vol.106, Rev.2, p.84-88.

4. S.S.Sagalov and A.N. Kostyuchenko. System of eddy-current testing of irradiated fuel rods for test facilities of inspection and repair of the VVER-1000 fuel assemblies. Transactions of FSUE "SSC RIAR", 2008. Issue 2, p. 8-15.

5. S.V.Amosov and S.V.Pavlov. "Equipement for non-destructive measurement of fuel-cladding gap". Voprosy Atomnoi Nauki i Tekhniki. Series "Material Science and New Materials", 1990, Issue 6(40), p.17-18.

6. S.V.Amosov and S.V.Pavlov. Specific features of the determination of the pellet-cladding gap of the fuel rods by nondestructive method. Advanced post-irradiation examination techniques for water reactor fuel. Proceedings of a Technical Committee meeting held Dimitrovgrad, Russian Federation, 14-18May, 2001 IAEA-TECDOC-1277, 2002 p.73-79.

7. A.N.Kostyuchenko. Facility for oxide film thickness measurement on the outer surface of spent VVER and rBMK fuel rods. New technologies for nuclear power engineering, industry and construction. Issue 4. Collected abstracts and works. SSC RIAR, Dimitrovgrad, 2001, p.38-42.

8. A.N.Kostyuchenko. Distribution of oxide film on the surface of cylindrical spent fuel assemblies VVER and RBMK. Atomnaya Energiya, Vol.102, Issue 6, 2007.